Current Research in Food Science 4 (2021) 821–828

Contents lists available at ScienceDirect

Current Research in Food Science

journal homepage: www.sciencedirect.com/journal/current-research-in-food-science

Unique distribution of ellagitannins in ripe strawberry fruit revealed by mass spectrometry imaging

Hirofumi Enomoto [a,b,c,*]

[a] Department of Biosciences, Faculty of Science and Engineering, Teikyo University, Utsunomiya, 320-8551, Japan
[b] Division of Integrated Science and Engineering, Graduate School of Science and Engineering, Teikyo University, Utsunomiya, 320-8551, Japan
[c] Advanced Instrumental Analysis Center, Teikyo University, Utsunomiya, 320-8551, Japan

ARTICLE INFO

Keywords:
Ellagitannin
Strawberry
Distribution
Mass spectrometry imaging
Matrix-assisted laser desorption/ionization
Liquid chromatography-mass spectrometry

ABSTRACT

Ellagitannins (ETs) are hydrolysable tannins composed of a polyol core, primarily glucose, which is esterified with hexahydroxydiphenic acid (HHDP), and in some cases, gallic acid. ETs are the major phenolic compounds found in strawberries and may contribute to the health-related properties of strawberries, because of their strong antioxidative activity. However, their distribution in the strawberry fruit remains unclear. In this study, matrix-assisted laser desorption/ionization-mass spectrometry imaging (MALDI–MSI) was used to visualize ETs in ripe strawberry fruits. Five peaks, corresponding to the *m/z* values of ET $[M-H]^-$ ions detected in the MALDI–MS spectrum of strawberry extracts, were identified as strictinin, pedunculagin, casuarictin, davuriicin M_1, and an unknown ET using MALDI–tandem MS (MS/MS). In addition, liquid chromatography–electrospray ionization–MS/MS of the extracts revealed the presence of pedunculagin isomers and the unknown ET. Ion images of these five ETs were reconstructed using MALDI–MSI. Strictinin was widely distributed in and around the achene seed coats, while the other ETs were dispersed in and around the seed coats, and at the bottom of the receptacle; pedunculagin was distributed in the epidermis and pith, whereas casuarictin, the unknown ET, and davuriicin M_1 were distributed in the pith. Moreover, MALDI–MSI of a casuarictin standard indicated that in-source fragmentation weakly affected the ion images. The results suggest that the distribution of ETs depends on the presence or absence of their constituents, namely galloyl units, HHDP, and bis-HHDP. To the best of my knowledge, this is the first report on the visualization of ETs in plant tissues using MSI, MALDI–MSI may be a useful tool for analyzing the distribution of ETs in the strawberry fruit.

1. Introduction

Strawberries (*Fragaria* × *ananassa* Duch.), in both fresh and processed forms, are the most widely consumed berries because of their appearance, taste, and health-related properties (Giampieri et al., 2014, 2015; Gunduz, 2016). Strawberries are rich in nutritive compounds, including sugars, organic acids, vitamins, and minerals, as well as a wide range of non-nutritive compounds, such as polyphenolic compounds (Giampieri et al., 2014, 2015; Gunduz, 2016). Hydrolysable tannins and flavonoids (primarily anthocyanins) are the major phenolic compounds in strawberries, followed by phenolic acids, and condensed tannins (proanthocyanidins) (Folmer et al., 2014; Giampieri et al., 2014, 2015; Gunduz, 2016).

Ellagitannins (ETs), the most abundant hydrolysable tannins found in the strawberry fruit (Giampieri et al., 2014), consist of a polyol core, typically glucose, which is esterified with hexahydroxydiphenic acid (HHDP), and in some cases, gallic acid (Aaby et al., 2007, 2012; Hannineva et al., 2008; Gasperotti et al., 2013; La Barbera et al., 2017; Czyżowska et al., 2020; Olennikov et al., 2020). ETs have anti-tumorigenic, anti-mutagenic, anti-diabetic, anti-proliferative, anti-bacterial, and antimycotic properties (Arapitsas, 2012; Folmer et al., 2014; Giampieri et al., 2014, 2015; Gunduz, 2016). Therefore, ETs from strawberry consumption are associated with the prevention of chronic diseases. Moreover, ETs may influence the shelf life of strawberries owing to their antioxidative and antimicrobial properties (Scalbert, 1991; Arapitsas, 2012). However, the spatial distribution of ETs in ripe

Abbreviations: CMC, carboxymethylcellulose; DAN, 1,5-diaminonaphthalene; ET, ellagitannin; HHDP, hexahydroxydiphenic acid; ITO, indium–tin oxide; LC, liquid chromatography; MALDI, matrix-assisted laser desorption/ionization; MSI, mass spectrometry imaging; RT, retention time; TOF, time-of-flight.

* Department of Biosciences, Faculty of Science and Engineering, Teikyo University, Utsunomiya, 320-8551, Japan.
E-mail address: enomoto@nasu.bio.teikyo-u.ac.jp.

https://doi.org/10.1016/j.crfs.2021.11.006
Received 29 June 2021; Received in revised form 12 November 2021; Accepted 12 November 2021
Available online 17 November 2021

strawberry fruits has not been elucidated. Thus, determining the distribution of ETs in strawberry fruit tissues is important to understand which tissues are crucial to harnessing its health-related properties.

Modern separation techniques, such as liquid chromatography–electrospray ionization–mass spectrometry (LC–ESI–MS), are widely used to analyze phenolic compounds such as ETs (Aaby et al., 2007, 2012; Hanhineva et al., 2008; Arapitsas, 2012; Gasperotti et al., 2013; La Barbera et al., 2017; Czyżowska et al., 2020; Olennikov et al., 2020). LC–ESI–tandem MS (MS/MS) has also been used to investigate the structural details and spatial distribution of ETs in different plant tissues. However, the spatial resolution of LC–ESI–MS/MS is dependent on the accuracy of sampling and tissue differentiation, preventing accurate observations. Recently, mass spectrometry imaging (MSI) has been modified using soft ionization techniques (Cooks et al., 2006; Wiseman et al., 2006; Cornett et al., 2007; Shimma et al., 2008; Setou et al., 2010; Nizioł et al., 2019; Enomoto et al., 2020a), such as matrix-assisted laser desorption/ionization (MALDI) (Li et al., 2007; Yoshimura et al., 2016; Crecelius et al., 2017; Enomoto et al., 2018, 2020b; Enomoto, 2020; Yoshimura and Zaima, 2020) and desorption ESI (Cabral et al., 2013; Wu et al., 2013; Enomoto, 2021; Enomoto and Miyamoto, 2021), to visualize various metabolites in food and plant tissues at the microscopic level without the use of antibodies, staining, or complicated preliminary procedures. MALDI–MSI has previously been used to visualize flavonoids, such as anthocyanins, flavan-3-ols, and flavonols, as well as ellagic acid-glycosides in strawberry fruits (Cabral et al., 2013; Crecelius et al., 2017; Enomoto et al., 2018, 2020b; Enomoto, 2020; Wang et al., 2021). Therefore, the aims of this study were to identify the ETs present in ripe strawberry fruits using MALDI–MS/MS and LC–ESI–MS/MS analyses and determine their spatial distribution using MALDI–MSI.

2. Materials and methods

2.1. Reagents

Strictinin and casuarictin were obtained from Nagara Science Co. Ltd. (Gifu, Japan); 1,5-diaminonaphthalene (DAN) from Tokyo Kasei Co. (Tokyo, Japan); cesium triiodide from Sigma-Aldrich Japan (St. Louis, MO, USA); indium–tin oxide (ITO)-coated glass slides (100 Ω without MAS coating) from Matsunami Glass Ind. (Osaka, Japan); water, methanol, acetonitrile, formic acid, and sodium salt of carboxymethylcellulose (CMC) from Fujifilm Wako Pure Chemicals Co. Ltd. (Tokyo, Japan). All reagents and solvents used in this study were of analytical grade.

2.2. Strawberry sampling

Fruits of the Japanese strawberry cultivar 'Tochiotome' were cultivated in the Strawberry Research Center, Tochigi, Japan. Twenty ripe strawberries were harvested from different plants, frozen with or without CMC freeze-embedding, and stored at −80 °C until use.

2.3. Preparation of strawberry crude extracts

Strawberry crude extracts were prepared by modifying previously described protocols (Enomoto et al., 2018, 2020b). Fresh strawberries were homogenized and freeze-dried; subsequently, the dry homogenate was dissolved in 80% methanol and centrifuged at 6300×*g* for 5 min. The supernatant was used as the crude extract for MALDI–MS/MS and LC–ESI–MS/MS analyses.

2.4. MALDI–MS and MS/MS analyses

MALDI–MS analyses were performed as previously described (Enomoto et al., 2018, 2020b), with minor modifications. The crude extract or ET standard solution was mixed with 1 μL of DAN solution (10 mg/mL in 80% aqueous methanol) on an ITO-coated glass slide, dried, and analyzed using the UltrafleXtreme MALDI time-of-flight (TOF)/TOF Mass Spectrometer (Bruker, Billerica, MA, USA) in the negative-ion and reflector modes. The mass ranges were measured at *m/z* 600–3000, and masses were calibrated externally using cesium triiodide.

For MS/MS analyses, the selected precursor and product ions were obtained using UltrafleXtreme in the collision-induced dissociation "LIFT" MS/MS mode. The *m/z* values of the precursor ions were set at ± 0.5%, and the MS/MS spectra were analyzed using FlexAnalysis 3.4 software (Bruker Daltonics, Bremen, Germany). ETs were identified by comparing their MS/MS spectra with those of the standards and with those in the published literature (Aaby et al., 2007, 2012; Hanhineva et al., 2008; Gasperotti et al., 2013; La Barbera et al., 2017; Czyżowska et al., 2020; Olennikov et al., 2020).

2.5. LC–ESI–MS and MS/MS analyses

LC–ESI–MS analyses were performed according to a previous study, with some modifications (Enomoto and Miyamoto, 2021). One microliter of the crude extract was injected into a Waters Acquity Ultra-Performance LC (UPLC) system (Waters Corp., Milford, MA, USA) coupled with a Synapt XS HDMS quadrupole-TOF mass spectrometer equipped with an ESI source (Waters Corp.) and an Acquity UPLC BEH C18 column (2.1 × 100 mm; particle size: 1.7 μm). The solvents used were water (solvent A) and acetonitrile (solvent B), each containing 0.1% formic acid. The LC gradient was set at a flow rate of 0.3 mL/min using the following concentrations of solvent B: 3% (0–1 min), 3–30% (1–10 min), 95% (10–13 min), and 3% (13–16 min). LC–ESI–MS spectra were obtained in the negative-ion and sensitivity modes at a mass resolution of approximately 20 000 FWHM over an *m/z* range of 500–1300 with a scan duration of 0.2 s in the centroid mode. The source parameters were set as follows: capillary: 2.0 kV; sampling cone: 20 V; source temperature: 120 °C; desolvation temperature: 450 °C; desolvation gas flow: 800 L/h. External and lock mass calibrations were applied using sodium formate and leucine enkephalin solutions (100 ppm; *m/z*: 554.26202 at 10 μL/min).

For MS/MS analyses, the ramp-trap collision energy was set at 20–40 V for strictinin, 20–50 V for pedunculagin, 20–60 V for casuarictin, 25–70 V for the unknown ET (*m/z* 1085.07), and 30–80 V for davuriicin M_1, while the transfer collision energy was set at 2 V for all the ETs. The *m/z* values of the precursor ions were set at ± 1.0 Da, and the data were analyzed using MassLynx 4.2 software (Waters Corp.).

2.6. Preparation of strawberry fruit sections

Fruit sections were prepared using CMC freeze-embedding, as previously described (Enomoto et al., 2018, 2020b). Longitudinal and cross sections (100 μm thick) of the CMC freeze-embedded fruits were prepared using a CM 1860 cryostat (Leica Microsystems, Wetzlar, Germany). The sections were then mounted onto ITO-coated glass slides and preserved at −80 °C until MALDI–MSI analyses were performed.

2.7. Matrix coating

Matrix vapor deposition and recrystallization were performed according to a previous study (Fujishima et al., 2021). First, 100 mg of DAN was vapor-deposited on the sections using a vacuum deposition system (SVC-700TMSG, Sanyu Electron Co. Ltd., Tokyo, Japan). Then, the sections were sprayed with 2 mL of DAN solution (5 mg/mL in 80% aqueous methanol) using an automatic matrix sprayer (iMatrixSpray, Tardo Gmbh, Switzerland) (Stoeckli et al., 2014). The spraying conditions were as follows: height, 80 mm; line distance, 2 mm; speed, 200 mm/s; density, 1 μL/cm^2; cycles, 15; delay, 0 s; dimensions, 100 × 50 mm^2; and bed temperature, 30 °C. Finally, the DAN on the section was exposed to the vapor in a semi-closed Petri dish for recrystallization.

2.8. MALDI–MSI analyses

MALDI–MSI analyses were performed according to a previous study, with minor modifications (Enomoto et al., 2018, 2020b). Strawberry fruit sections were analyzed using UltrafleXtreme in the negative-ion and reflector modes. The instrumental conditions were set as follows: step size: 200 μm; *m/z* range: 600–1300; laser diameter: medium. Mass calibration was performed externally using cesium triiodide, and the spectra were obtained automatically using FlexImaging 4.1 software (Bruker Daltonics). The spectra were normalized using the same software based on the total ion count and reconstructed ion images.

To determine the spatial distribution of the identified ETs, three different strawberry fruits were analyzed. For the analysis of the strictinin and casuarictin standards, each standard solution (50 ng/μL) was mixed with DAN solution on an ITO-coated glass slide.

3. Results and discussion

3.1. MALDI–MS/MS analyses of ETs in the strawberry crude extract

ETs in various plants have been analyzed using the negative-ion mode of LC–ESI–MS/MS, and several ET species have been reported, particularly in strawberries (Aaby et al., 2007, 2012; Hanhineva et al., 2008; Gasperotti et al., 2013; La Barbera et al., 2017; Czyżowska et al., 2020; Olennikov et al., 2020). Therefore, strawberry crude extracts were prepared and an *m/z* range of 600–3000 was analyzed to determine whether ETs can be detected using the negative-ion mode of MALDI–MS.

Within the 600–1300 *m/z* range, five peaks (*m/z* 633.1, 783.1, 935.1, 1085.1, and 1235.1) corresponding to the previously reported *m/z* values of ET $[M–H]^-$ ions were detected (Fig. 1a) (Aaby et al., 2007, 2012; Hanhineva et al., 2008; Gasperotti et al., 2013; La Barbera et al.,

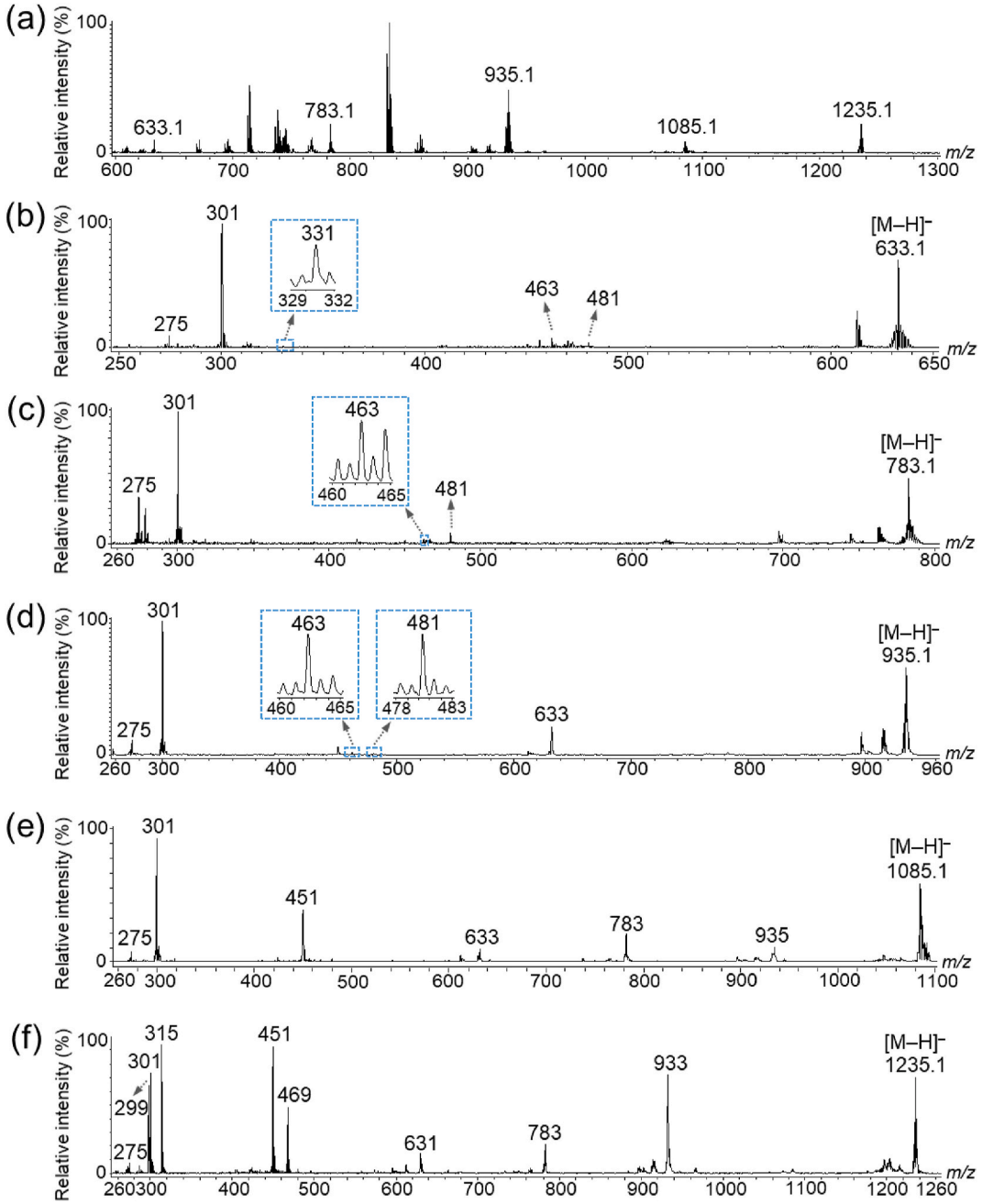

Fig. 1. Matrix-assisted laser desorption/ionization-mass spectrometry (MALDI–MS) and tandem MS (MS/MS) analyses of strawberry fruit extracts. (a) MS spectra at *m/z* 600–1300. MS/MS spectra of the precursor ions at *m/z* (b) 633.1, (c) 783.1, (d) 935.1, (e) 1085.1, and (f) 1235.1.

2017; Czyżowska et al., 2020; Olennikov et al., 2020). Previous studies revealed that agrimoniin is one of the most abundant ETs in *F. ananassa* Duch. (Giampieri et al., 2014; Gunduz, 2016). However, in this study, the peak at *m/z* 1869.1, corresponding to the agrimoniin $[M–H]^-$ ion, was only marginally detected in the crude extract.

To verify whether the five peaks corresponded to ETs, the peaks were analyzed using MALDI–MS/MS. Typical losses during fragmentation include galloyl (152 amu), HHDP (302 amu), galloylglucose (332 amu), HHDP-glucose (482 amu), and galloyl-HHDP-glucose (634 amu) (Arapitsas, 2012). Moreover, an HHDP moiety is present in ET when a fragment ion corresponds to a peak at *m/z* 301. In the MS/MS spectrum of the precursor ion at *m/z* 633.1, fragment ion peaks were detected at *m/z* 481 (−152, loss of gallic acid), 331 (−302, loss of HHDP), and 301 (Fig. 1b). This fragmentation pattern was similar to that of the galloyl-HHDP-glucose (strictinin) standard (Supplementary Fig. S1a). In addition, previous reports indicated that *m/z* 633.1 in strawberries corresponded to strictinin $[M–H]^-$ ions (Aaby et al., 2007, 2012; Hanhineva et al., 2008; Gasperotti et al., 2013; La Barbera et al., 2017; Czyżowska et al., 2020; Olennikov et al., 2020). Therefore, the peak at *m/z* 633.1 was designated as strictinin $[M–H]^-$ ions (Table 1, and Supplementary Fig. S2a).

In contrast, the fragment ion peaks for the MS/MS spectrum at *m/z* 783.1 were detected at *m/z* 481 (−302, loss of HHDP) and 301 (−482, loss of HHDP-glucose) (Fig. 1c), indicating that *m/z* 783.1 was bis-HHDP-glucose (pedunculagin) (Table 1, and Supplementary Fig. S2b) (Aaby et al., 2007; Hanhineva et al., 2008). In the MS/MS spectrum at *m/z* 935.1, the fragment ion peaks were detected at *m/z* 633 (−302, loss of HHDP) and 301 (Fig. 1d). This fragmentation pattern had been previously reported and is similar to that of the galloyl-bis-HHDP-glucose (casuarictin) standard (Supplementary Fig. S1b) (Aaby et al., 2007, 2012; Hanhineva et al., 2008; Gasperotti et al., 2013; La Barbera et al., 2017; Czyżowska et al., 2020; Olennikov et al., 2020), indicating that the peak at *m/z* 935.1 corresponded to casuarictin (Table 1, and Supplementary Fig. S2c). However, in the MS/MS spectrum at *m/z* 1085.1, the fragment ion peaks were detected at *m/z* 935, 783, 633, 451, and 301 (Fig. 1e), similar to those of an unknown ET or a putative galloyl-castalagin (Table 1) (Hanhineva et al., 2008; Gasperotti et al., 2013). Moreover, in the MS/MS spectrum at *m/z* 1235.1, the fragment ion peaks were detected at *m/z* 933 (−302, loss of HHDP), 783, 631 (−302, loss of two HHDP), 469, 451, 315, 301 (loss of 934 amu), and 299 (Fig. 1f), suggesting that this peak corresponded to an ET containing a dilactonized sanguisorboyl group and could be bis-HHDP-glucose-galloyl-ellagic acid (davuriicin M_1) (Table 1) (Hanhineva et al., 2008; Aaby et al., 2012; Gasperotti et al., 2013; Czyżowska et al., 2020).

Table 1
Ellagitannins (ETs) identified in strawberry fruit extract using MALDI–MS and MS/MS analyses.

Molecular species (Structure)	Chemical formula	Exact *m/z*, $[M–H]^-$	Detected *m/z*, $[M–H]^-$	Fragment ions for assignment, *m/z*
Strictinin (Galloyl-HHDP-glucose)	$C_{27}H_{22}O_{18}$	633.0733	633.1	481, 463, 301, 275
Pedunculagin (bis-HHDP-glucose)	$C_{34}H_{24}O_{22}$	783.0686	783.1	633, 481, 463, 301, 275
Casuarictin (galloyl-bis-HHDP-glucose)	$C_{41}H_{28}O_{26}$	935.0796	935.1	633, 481, 463, 301, 275
Unknown ET	$C_{48}H_{30}O_{30}$	1085.0749	1085.1	935, 783, 633, 451, 301, 275
Davuriicin M_1 (bis-HHDP-glucose-galloyl-ellagic acid)	$C_{55}H_{32}O_{34}$	1235.0702	1235.1	933, 783, 631, 469, 451, 315, 301, 299, 275

HHDP, hexahydroxydiphenic acid.
Pedunculagin and davuriicin M_1 were tentatively identified.

3.2. LC–ESI–MS/MS analyses of ETs in the strawberry extract

Previous studies suggest that there are several isomers of each ET in the strawberry fruit (Aaby et al., 2007, 2012; Hanhineva et al., 2008; Gasperotti et al., 2013; La Barbera et al., 2017; Czyżowska et al., 2020; Olennikov et al., 2020). Therefore, to determine the isomers of the ETs identified in the crude extract, LC–ESI–MS/MS was performed. Although ETs have been reported as both $[M–H]^-$ and $[M–2H]^{2-}$ ions (Arapitsas, 2012), the MS/MS analyses were performed only for $[M–H]^-$ ions because all the ETs detected using MALDI–MS were $[M–H]^-$ ions.

The LC–ESI–MS/MS fragmentation patterns of the ETs were similar to those of the MALDI–MS/MS spectra. The retention time (RT) of the peak at *m/z* 633.0765 was 5.4 min, which was the same as that of the strictinin standard (Fig. 2a, Table 2, and Supplementary Fig. S3a), suggesting that the peak at *m/z* 633.1 corresponded to strictinin (Table 1). However, for the peak at *m/z* 783.0629, with a fragmentation pattern corresponding to that of pedunculagin, the RTs were 3.6 and 4.7 min, suggesting that this peak corresponded to pedunculagin or its isomers (Fig. 2b and c, and Tables 1 and 2). The peak at *m/z* 935.0822 corresponded to casuarictin, with an RT of 6.8 min (Fig. 2d, Tables 1 and 2, and Supplementary Fig. S3b). The RTs of the peaks at *m/z* 1085.0743 and 1235.0692, with fragmentation patterns corresponding to the unknown ET and davuriicin M_1, respectively, were 8.3, 8.4, and 9.5 for the unknown ET and 6.7 min for davuriicin M_1, suggesting that the peaks at *m/z* 1085.1 and 1235.1 corresponded to the unknown ET and its isomers, or davuriicin M_1, respectively (Fig. 2e–h and Tables 1 and 2).

3.3. MALDI–MSI analyses of ETs in the strawberry fruit sections

The flesh of the strawberry fruit is a swollen receptacle (false fruit), while the seeds or achenes at the surface of the receptacle are the true fruits. They are collectively referred to as the strawberry fruit (Giampieri et al., 2014, 2015). Thus, to determine the spatial distribution of the identified ETs in the strawberry fruit (Table 1), longitudinal and cross sections of three different 'Tochiotome' strawberries obtained from different plants were analyzed using MALDI–MSI. Several tissues, including the achenes, were observed in the longitudinal sections of the strawberry fruit (Fig. 3a, Supplementary Fig. S4), and all five peaks corresponding to the ETs identified in the strawberry extracts were detected in the MALDI–MSI spectra of the sections (Fig. 3b). Furthermore, ion images of the ETs were reconstructed to determine their distributions, and distinct ET distribution patterns were observed among different tissues. Representative ion images of one of the three fruits are shown in Fig. 3; ion images of the other two fruits are shown in Supplementary Fig. S4. The ETs showed similar distribution patterns among these fruits. Strictinin was widely distributed in and around the achene seed coat (Fig. 3c), while pedunculagin or its isomers were primarily distributed in and around the achene seed coat and in the epidermis and pith tissue at the bottom of the receptacle (Fig. 3d). In contrast, casuarictin and davuriicin M_1 were uniformly distributed in and around the achene seed coat and in the pith tissue at the bottom of the receptacle (Fig. 3e and g). Although the unknown ET had a similar distribution to casuarictin and davuriicin M_1, it was more abundant in the pith tissue than in the achene seed coat (Fig. 3f).

Strictinin includes an HHDP in its structure, while both casuarictin and davuriicin M_1 consist of a bis-HHDP moiety (Table 1), suggesting that ETs with an HHDP were only present in and around the achene seed coat, while those with bis-HHDP were present at the bottom of the receptacle as well as in and around the achene seed coat. In contrast to casuarictin and davuriicin M_1, pedunculagin has no galloyl unit (Table 1), suggesting that at the bottom of the receptacle, the ETs with bis-HHDP and without galloyl units were distributed in the epidermis and pith tissue, while those with both bis-HHDP and galloyl units were dispersed in the pith tissue. These results suggest that the distribution patterns of ETs in the strawberry fruit depend on the presence or absence of their constituents, namely galloyl units, HHDP, and bis-HHDP.

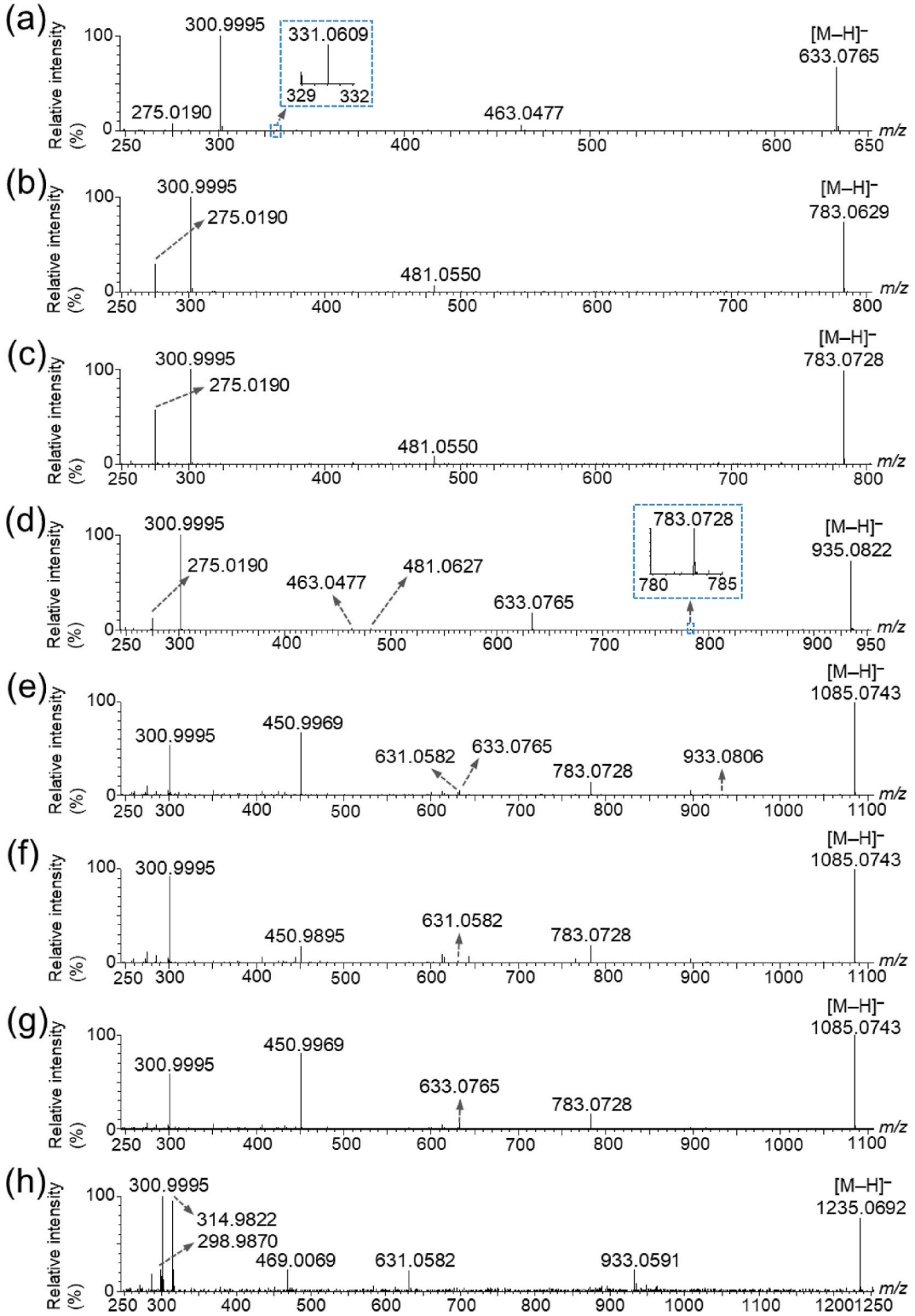

Fig. 2. Liquid chromatography–electrospray ionization–tandem mass spectrometry (LC–ESI–MS/MS) analysis of ellagitannins in strawberry fruit extracts. MS/MS spectra of the precursor ions (a) at *m/z* 633.1, and at *m/z* 783.1 with retention times (RTs) of (b) 3.6 min and (c) 4.7 min, respectively, (Table 2), (d) at *m/z* 935.1, and at *m/z* 1085.1 with RTs of (e) 8.3 min, (f) 8.4 min, (g) 9.5 min (Table 2), and (h) 1235.1 ± 1 Da, respectively.

Previous studies suggest that MALDI–MSI of flavonoids and ellagic acid-glycosides in strawberry fruits results in in-source fragmentation (Enomoto et al., 2018, 2020b; Enomoto, 2020). The analysis of flavan-3-ols revealed that robust in-source fragmentation affected the ion images because the *m/z* values of the fragment ions generated from the larger polymerized ions were the same as that of the smaller polymerized ions (Enomoto et al., 2020b). Therefore, to investigate the effects of in-source fragmentation on the ion images of ETs, a casuarictin standard was analyzed using MALDI–MSI. Although the detection intensities of *m/z* 633.1 and 783.1 were 13.5 and 9.5 times lower than that of *m/z* 935.1, the peaks detected at *m/z* 935.1, 783.1, and 633.1 corresponded to casuarictin, strictinin, and pedunculagin $[M–H]^-$ ions,

Table 2
Ellagitannins (ETs) identified in strawberry fruit extract using LC–ESI–MS and MS/MS analyses.

Molecular species	RT (min)	Detected *m/z*, $[M–H]^-$	Error (ppm)	Fragment ions for assignment (*m/z*)
Strictinin	5.4	633.0765	+5.1	481.0627, 463.0477, 300.9995, 275.0190
Pedunculagin or its isomers	3.6 4.7	783.0629 783.0629	−7.3 −7.3	481.0627, 300.9995, 275.0190 481.0550, 300.9995, 275.0190
Casuarictin	6.8	935.0822	+2.8	783.0728, 633.0765, 481.0550, 463.0553, 300.9995, 275.0190
Unknown ET or its isomers	8.3 8.4 9.5	1085.0743 1085.0743 1085.0743	−0.6 −0.6 −0.6	783.0728, 633.0765, 450.9969 300.9995 783.0728, 631.0582, 450.9895, 300.9995 783.0728, 633.0765, 450.9969, 300.9995
Davuriicin M_1, or its isomer	6.7	1235.0692	−0.8	933.0591, 631.0582, 469.0069, 314.9822, 300.9995, 298.9870

RT: retention time.
Pedunculagin and davuriicin M_1 were tentatively identified.

respectively, suggesting that in-source fragmentation of ETs occurred during MALDI–MSI (Fig. 4). In addition, the distribution patterns of the identified ETs were not identical, suggesting a weak influence of in-source fragmentation on the ion images of ETs.

Recently, strawberry extracts containing phenolic compounds have been used as ingredients in functional foods and dietary supplements in combination with other fruits, vegetables, and herbal extracts (Giampieri et al., 2014, 2015; Gunduz, 2016). Although the distribution patterns of phenolic compounds differed among molecular species, these studies revealed their distributions in ripe strawberry fruits. Anthocyanins were detected in the achene seed coats, epidermis, and cortical and pith tissues (Enomoto et al., 2018); flavan-3-ols were detected in the bottom of the receptacle, in and around the vascular bundles, and in the epidermis (Enomoto et al., 2020b); flavonols were detected in the epidermis, while ellagic acid-glycosides were found in the achenes and at the bottom of the receptacle, similar to ETs (Enomoto et al., 2020a). The present study found a unique accumulation of ETs in and around the achene seed coat and at the bottom of the receptacle. These findings will aid in the development of better strategies for the preparation of strawberry extracts enriched with specific phenolic compounds. Although ETs are considered therapeutic for chronic diseases owing to their strong antioxidative properties (Arapitsas, 2012; Folmer et al., 2014; Giampieri et al., 2014, 2015; Gunduz, 2016), the relationship between their preventive effects for chronic diseases and their structural differences has not been sufficiently investigated owing to the limited number of commercially available ET standards (Arapitsas, 2012). This

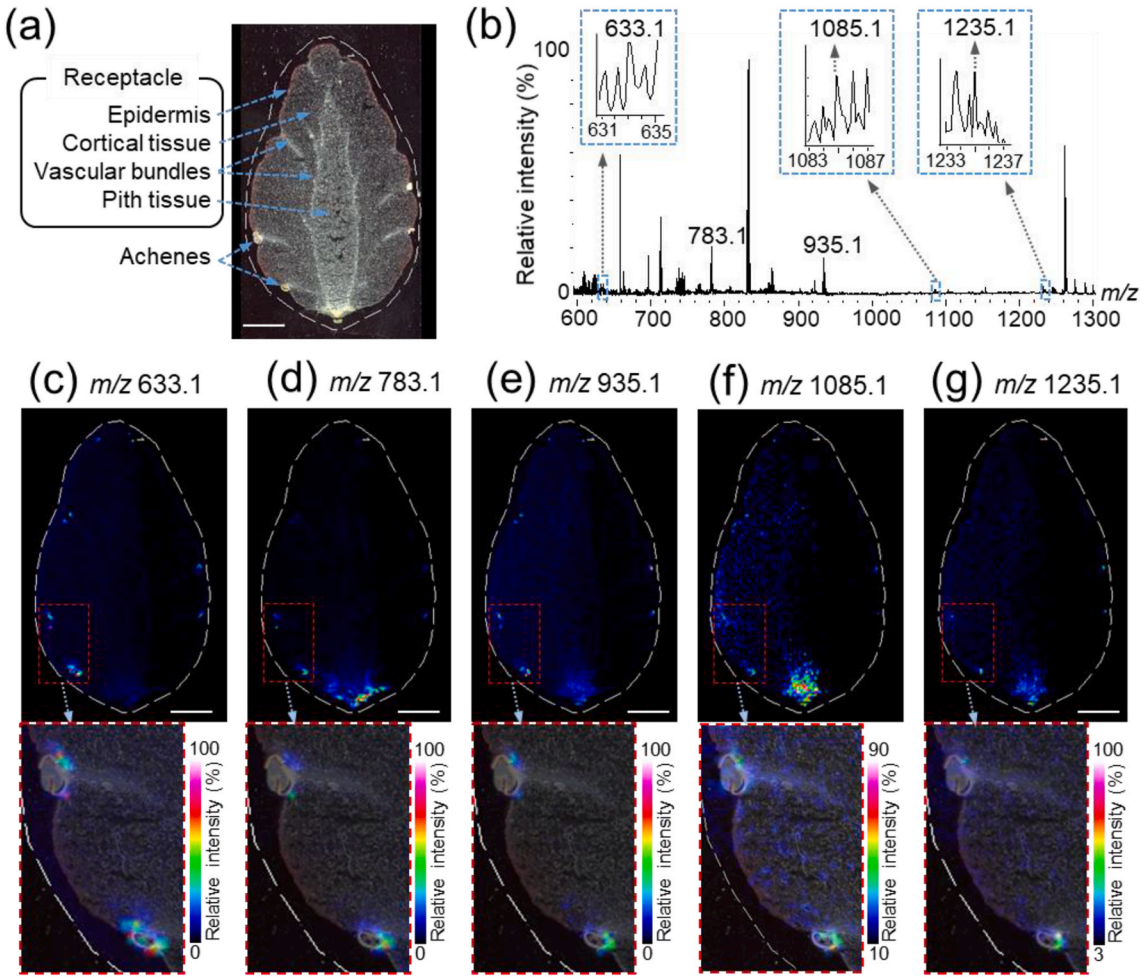

Fig. 3. Matrix-assisted laser desorption/ionization-mass spectrometry imaging (MALDI–MSI) analysis of the strawberry fruit sections. (a) Optical image of an analyzed section. (b) Mass spectrum of the section. Ion images at *m/z* (c) 633.1, (d) 783.1, (e) 935.1, (f) 1085.1, and (g) 1235.1. The dotted white line shows the analyzed region. Scale bar = 5 mm.

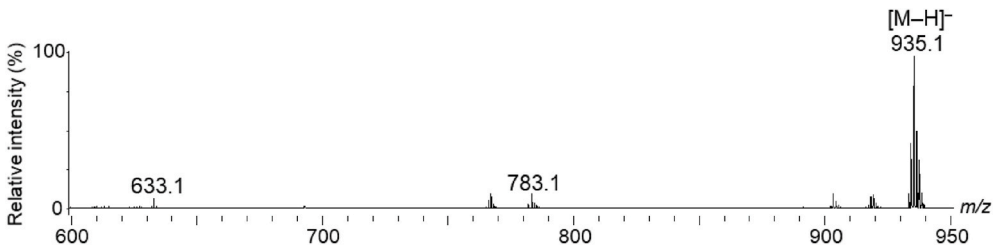

Fig. 4. Mass spectrum of the casuarictin standard obtained using Matrix-assisted laser desorption/ionization-mass spectrometric imaging (MALDI–MSI).

study also contributes to the purification of a specific ET for medicinal or research purposes.

Similar to flavan-3-ols, tannins are toxic to bacteria (Scalbert, 1991). Nizioł et al. (2019) visualized flavan-3-ols in strawberry fruits using MSI with ^{109}Ag nanoparticle-enhanced targets and reported that their distribution was related to their protective function. Pathogens, such as bacteria, infect plant surface tissues, such as the epidermis, and proliferate in the infected tissues, spreading throughout the plant body via the vascular bundles. Therefore, the unique distribution of each ET might reveal its protective role during infection and the spread of pathogens in the tissues of ripe strawberry fruits (Enomoto et al., 2020b).

Ongoing investigations aim to improve the food quality traits of the strawberry fruit, such as its health-related properties and resistance to biotic and abiotic stresses through genetic manipulation (Giampieri et al., 2014, 2015; Gunduz, 2016). Distribution analyses of ETs among strawberry cultivars using MALDI–MSI would help breeders to improve the health-related properties of strawberries more rapidly. Furthermore, the MALDI–MSI analysis used in this study can be used for the distribution analyses of ETs in other plant species and tissues.

4. Conclusions

To the best of my knowledge, this is the first report on the visualization of ETs in plant tissues using MSI. In this study, five ETs and their isomers were identified in the strawberry fruit using MALDI–MS/MS and LC–ESI–MS/MS. The distribution of each ET was dependent on its constituents. However, the isomers of each ET could not be visualized, because they had the same *m/z* values and similar fragmentation patterns. Therefore, further improvements are needed in the analytical methodologies to investigate the detailed distribution pattern of each ET. Nonetheless, MALDI–MSI is a valuable tool for the distribution analysis of ETs in the strawberry fruit, which will provide novel insights into the fields of food and plant sciences.

Financial support

This work was supported by ACRO Research Grants of Teikyo University (H. Enomoto).

CRediT authorship contribution statement

Hirofumi Enomoto: Conceptualization, Methodology, Validation, Formal analysis, Investigation, Resources, Writing – original draft, Writing – review & editing, Visualization, Funding acquisition.

Declaration of competing interest

The authors declare that they have no known competing financial interests or personal relationships that could have appeared to influence the work reported in this paper.

Acknowledgments

The author gratefully acknowledges Dr. Yukio Inaba and Mr. Tatsuhiro Ienaka (Strawberry Research Center of the Tochigi Prefectural Agricultural Experiment Station) for providing the 'Tochiotome' strawberry fruit samples used. The author gratefully acknowledge Editage (www.editage.jp) for English language editing.

Appendix A. Supplementary data

Supplementary data to this article can be found online at https://doi.org/10.1016/j.crfs.2021.11.006.

References

Aaby, K., Ekeberg, D., Skrede, G., 2007. Characterization of phenolic compounds in strawberry (*Fragaria* x *ananassa*) fruits by different HPLC detectors and contribution of individual compounds to total antioxidant capacity. J. Agric. Food Chem. 55, 4395–4406. https://doi.org/10.1021/jf0702592.

Aaby, K., Mazur, S., Nes, A., Skrede, G., 2012. Phenolic compounds in strawberry (*Fragaria* x *ananassa* Duch.) fruits: composition in 27 cultivars and changes during ripening. Food Chem. 132, 86–97. https://doi.org/10.1016/j.foodchem.2011.10.037.

Arapitsas, P., 2012. Hydrolyzable tannin analysis in food. Food Chem. 135, 1708–1717. https://doi.org/10.1016/j.foodchem.2012.05.096.

Cabral, E.C., Mirabelli, M.F., Perez, C.J., Ifa, D.R., 2013. Blotting assisted by heating and solvent extraction for DESI-MS imaging. J. Am. Soc. Mass Spectrom. 24, 956–965. https://doi.org/10.1007/s13361-013-0616-y.

Cooks, R.G., Ouyang, Z., Takats, Z., Wiseman, J.M., 2006. Ambient mass spectrometry. Science 311, 1566–1570. https://doi.org/10.1126/science.1119426.

Cornett, D.S., Reyzer, M.L., Chaurand, P., Caprioli, R.M., 2007. MALDI imaging mass spectrometry: molecular snapshots of biochemical systems. Nat. Methods 4, 828–833. https://doi.org/10.1038/nmeth1094.

Crecelius, A.C., Hölscher, D., Hoffmann, T., Schneider, B., Fischer, T.C., Hanke, M.V., Flachowsky, H., Schwab, W., Schubert, U.S., 2017. Spatial and temporal localization of flavonoid metabolites in strawberry fruit (*Fragaria* × *ananassa*). J. Agric. Food Chem. 65, 3559–3568. https://doi.org/10.1021/acs.jafc.7b00584.

Czyżowska, A., Wilkowska, A., Staszczak Mianowska, A., Nowak, A., 2020. Characterization of phytochemicals in berry fruit wines analyzed by liquid chromatography coupled to photodiode-array detection and electrospray ionization/ion trap mass spectrometry (LC-DAD-ESI-MS^n) and their antioxidant and antimicrobial activity. Foods 9, 1783. https://doi.org/10.3390/foods9121783.

Enomoto, H., 2020. Mass spectrometry imaging of flavonols and ellagic acid glycosides in ripe strawberry fruit. Molecules 25, 4600. https://doi.org/10.3390/molecules25204600.

Enomoto, H., 2021. Adhesive film applications help to prepare strawberry fruit sections for desorption electrospray ionization-mass spectrometry imaging. Biosci. Biotechnol. Biochem. 85, 1341–1347. https://doi.org/10.1093/bbb/zbab033.

Enomoto, H., Kotani, M., Ohmura, T., 2020a. Novel blotting method for mass spectrometry imaging of metabolites in strawberry fruit by desorption/ionization using through hole alumina membrane. Foods 9, 408. https://doi.org/10.3390/foods9040408.

Enomoto, H., Miyamoto, K., 2021. Unique localization of jasmonic acid-related compounds in developing *Phaseolus vulgaris* L. (common bean) seeds revealed through desorption electrospray ionization-mass spectrometry imaging. Phytochemistry 188, 112812. https://doi.org/10.1016/j.phytochem.2021.112812.

Enomoto, H., Sato, K., Miyamoto, K., Ohtsuka, A., Yamane, H., 2018. Distribution analysis of anthocyanins, sugars, and organic acids in strawberry fruits using matrix-assisted laser desorption/ionization-imaging mass spectrometry. J. Agric. Food Chem. 66, 4958–4965. https://doi.org/10.1021/acs.jafc.8b00853.

Enomoto, H., Takahashi, S., Takeda, S., Hatta, H., 2020b. Distribution of flavan-3-ol species in ripe strawberry fruit revealed by matrix-assisted laser desorption/ionization-mass spectrometry imaging. Molecules 25, 103. https://doi.org/10.3390/molecules25010103.

Folmer, F., Basavaraju, U., Jaspars, M., Hold, G., El-Omar, E., Dicato, M., Diederich, M., 2014. Anticancer effects of bioactive berry compounds. Phytochemistry Rev. 13, 295–322. https://doi.org/10.1007/s11101-013-9319-z.

Fujishima, R., Kugo, H., Yanagimoto, K., Enomoto, H., Moriyama, T., Zaima, N., 2021. Similar distribution of orally administered eicosapentaenoic acid and M_2

macrophage marker in the hypoperfusion-induced abdominal aortic aneurysm wall. Food Funct 12, 3469–3475. https://doi.org/10.1039/d0fo03317k.
Gasperotti, M., Masuero, D., Guella, G., Palmieri, L., Martinatti, P., Pojer, E., Mattivi, F., Vrhovsek, U., 2013. Evolution of ellagitannin content and profile during fruit ripening in *Fragaria* spp. J. Agric. Food Chem. 61, 8597–8607. https://doi.org/10.1021/jf402706h.
Giampieri, F., Alvarez-Suarez, J.M., Battino, M., 2014. Strawberry and human health: effects beyond antioxidant activity. J. Agric. Food Chem. 62, 3867–3876. https://doi.org/10.1021/jf405455n.
Giampieri, F., Forbes-Hernandez, T.Y., Gasparrini, M., Alvarez-Suarez, J.M., Afrin, S., Bompadre, S., Quiles, J.L., Mezzettia, B., Battino, M., 2015. Strawberry as a health promoter: an evidence based review. Food Funct 6, 1386–1398. https://doi.org/10.1039/c5fo00147a.
Gunduz, K., 2016. Strawberry: phytochemical composition of strawberry (*Fragaria* x *ananassa*). In: Simmonds, M.S.J., Preedy, V.R. (Eds.), Nutritional Composition of Fruit Cultivars. Academic Press, San Diego, CA, USA, pp. 733–752. https://doi.org/10.1016/B978-0-12-408117-8.00030-1.
Hanhineva, K., Rogachev, I., Kokko, H., Mintz-Oron, S., Venger, I., Karenlampi, S., Aharoni, A., 2008. Non-targeted analysis of spatial metabolite composition in strawberry (*Fragaria* x *ananassa*) flowers. Phytochemistry 69, 2463–2481. https://doi.org/10.1016/j.phytochem.2008.07.009.
La Barbera, G., Capriotti, A.L., Cavaliere, C., Piovesana, S., Samperi, R., Chiozzi, R.Z., Laganà, A., 2017. Comprehensive polyphenol profiling of a strawberry extract (*Fragaria ananassa*) by ultra-high-performance liquid chromatography coupled with high-resolution mass spectrometry. Anal. Bioanal. Chem. 409, 2127–2142. https://doi.org/10.1007/s00216-016-0159-8.
Li, Y., Shrestha, B., Vertes, A., 2007. Atmospheric pressure molecular imaging by infrared MALDI mass spectrometry. Anal. Chem. 79, 523–532. https://doi.org/10.1021/ac061577n.
Nizioł, J., Misiorek, M., Ruman, T., 2019. Mass spectrometry imaging of low molecular weight metabolites in strawberry fruit (*Fragaria* x *ananassa* Duch.) cv. Primoris with ^{109}Ag nanoparticle enhanced target. Phytochemistry 159, 11–19. https://doi.org/10.1016/j.phytochem.2018.11.014.
Olennikov, D.N., Vasilieva, A.G., Chirikova, N.K., 2020. *Fragaria viridis* fruit metabolites: variation of LC-MS profile and antioxidant potential during ripening and storage. Pharmaceuticals 13, 262. https://doi.org/10.3390/ph13090262.
Scalbert, A., 1991. Antimicrobial properties of tannins. Phytochemistry 30, 3875–3883. https://doi.org/10.1016/0031-9422(91)83426-L.
Setou, M., Shrivas, K., Sroyraya, M., Yang, H., Sugiura, Y., Moribe, J., Kondo, A., Tsutsumi, K., Kimura, Y., Kurabe, N., Hayasaka, T., Goto-Inoue, N., Zaima, N., Ikegami, K., Sobhon, P., Konishi, Y., 2010. Developments and applications of mass microscopy. Med. Mol. Morphol. 43, 1–5. https://doi.org/10.1007/s00795-009-0489-0.
Shimma, S., Sugiura, Y., Hayasaka, T., Zaima, N., Matsumoto, M., Setou, M., 2008. Mass imaging and identification of biomolecules with MALDI-QIT-TOF-based system. Anal. Chem. 80, 878–885. https://doi.org/10.1021/ac071301v.
Stoeckli, M., Staab, D., Wetzel, M., Brechbuehl, M., 2014. IMatrixSpray: a free and open source sample preparation device for mass spectrometric imaging. Chimia 68, 146–149. https://doi.org/10.2533/chimia.2014.146.
Wang, J., Yang, E., Chaurand, P., Raghavan, V., 2021. Visualizing the distribution of strawberry plant metabolites at different maturity stages by MALDI-TOF imaging mass spectrometry. Food Chem. 345, 128838. https://doi.org/10.1016/j.foodchem.2020.128838.
Wiseman, J.M., Ifa, D.R., Song, Q., Cooks, R.G., 2006. Tissue imaging at atmospheric pressure using Desorption Electrospray Ionization (DESI) mass spectrometry. Angew. Chem. Int. Ed. 45, 7188–7192. https://doi.org/10.1002/anie.200602449.
Wu, C., Dill, A.L., Eberlin, L.S., Cooks, R.G., Ifa, D.R., 2013. Mass spectrometry imaging under ambient conditions. Mass Spectrom. Rev. 32, 218–243. https://doi.org/10.1002/mas.21360.
Yoshimura, Y., Zaima, N., 2020. Application of mass spectrometry imaging for visualizing food components. Foods 9, 575. https://doi.org/10.3390/foods9050575.
Yoshimura, Y., Goto-Inoue, N., Moriyama, T., Zaima, N., 2016. Significant advancement of mass spectrometry imaging for food chemistry. Food Chem. 210, 200–211. https://doi.org/10.1016/j.foodchem.2016.04.096.